

Supporting Information

Customizing Dumbbell-shaped Heterostructured Artificial Photosystems Steering Versatile Photoredox Catalysis

Peng Su^a, Xian Yan^a, Fang-Xing Xiao^{a, b*}

a. College of Materials Science and Engineering, Fuzhou University, New Campus, Minhou, Fujian
Province, 350108, China.

b. State Key Laboratory of Structural Chemistry, Fujian Institute of Research on the Structure of Matter,
Chinese Academy of Sciences, Fuzhou, Fujian 350002, PR China.

E-mail: fxxiao@fzu.edu.cn

Table of Contents

Page NO.

Experimental section	S3
Figure S1. XRD patterns of CdS, CM ^x , MoS ₂ and CM ² C ¹	S5
Figure S2. Survey spectrum of CdS and CM ² C ¹	S6
Figure S3. BET results of CdS, CM ² and CM ² C ¹ nanocomposite.....	S7
Figure S4. Schematic diagram of photoelectron transfer over the CdS/MoS ₂ /CuS, C-C-M, C/C/M.....	S8
Figure S5. Photoactivities of CM ² C ¹ under different light intensity.....	S9
Figure S6. XRD spectra of CM ² C ¹ nanocomposite of before and after cyclic reaction.....	S10
Figure S7. Raman spectra of CM ² C ¹ nanocomposite of before and after cyclic reaction.....	S11
Figure S8. SEM spectra of CM ² C ¹ nanocomposite of after cyclic reaction.....	S12
Figure S9. XPS spectrum of CM ² C ¹ nanocomposite of before and after cyclic reaction.....	S13
Figure S10. Blank experiments for photocatalytic reduction of 4-NA without catalyst or light.....	S14
Figure S11. Photoactivities of CdS, C-C-M, CM ² C ¹ towards the photoreduction of other nitroaromatics.....	S15
Figure S12. Photoactivities of CdS, C/C/M, CM ² C ¹ towards the photoreduction of other nitroaromatics.....	S16
Figure S13. Photoactivities of CM ² C ¹ towards photoreduction of 4-NA with and without adding AgNO ₃	S17
Figure S14. SEM images of CMA.....	S18
Figure S15. HRTEM images of CMA.....	S19
Figure S16. XPS spectrum of CMA.....	S20
Figure S17. The hydrogen evolution of CdS, CM ² and CMA.....	S21
Figure S18. XRD spectra of CMA nanocomposite of before and after cyclic reaction.....	S22
Figure S19. Raman spectra of CMA nanocomposite of before and after cyclic reaction.....	S23
Figure S20. PEC results of CdS, CM ² and CMA under visible light ($\lambda > 420$ nm) irradiation.....	S24
Figure S21. Energy band characterization of CdS.....	S25
Figure S22. Energy band characterization of CuS.....	S26
Figure S23. Energy band diagram of the CdS/CuS heterostructure before and after contact.....	S27
Figure S24. Schematic illustration of the photocatalytic mechanism of CdS/MoS ₂ /CuS heterostructure.....	S28
Table S1. Peak position with corresponding functional groups for all photoanodes.....	S29
Table S2. Chemical bond species for CdS, CM ² and CM ² C ¹ nanocomposite.....	S30
Table S3. Specific surface area, pore volume and pore size of CdS, CM ² and CM ² C ¹	S31

Table S4. Comparison of photocatalytic activity with reported CdS-based photocatalysts.....	S32
Table S5. Chemical bond species for CdS, CM ² and CMA nanocomposite.....	S33
References	S34

Experimental Section

1. Materials

The following chemicals were used as received without further purification: All chemicals were used without further purification. Deionized water (DI H₂O, Millipore, 18.2 MΩ cm resistivity) was used for all experiments. Cadmium acetate (C₄H₆CdO₄·2H₂O), thioacetamide (CH₄N₂S), ethylenediamine (EDA), diethylenetriamine (DETA), sodium molybdate (Na₂MoO₄·2H₂O), silver nitrate (AgNO₃), Copper chloride (CuCl₂·2H₂O). Above-mentioned all materials were directly employed without further purification.

2. Preparation of CdS nanowires (NWs)

CdS nanowires were prepared by the solvothermal method. In a typical synthesis step, 2.8 g of cadmium acetate C₄H₆CdO₄·2H₂O was dissolved in 50 mL of ethylenediamine. Then 1.4 g of CH₄N₂S was added to the solution and stirred again for about 1 h. After transferring to the reactor, it was kept at 160 °C for 18 h. The obtained precipitate was washed with distilled water and ethanol 3 times or more and finally dried in an oven at 60 °C overnight.^[1]

3. Preparation of CdS/MoS₂ nanodumbbell binary nanocomposite

0.125 g of the previously synthesized cadmium sulfide was dispersed in 20 mL of diethylenetriamine and 4 mL of water. After 15 min of ultrasonic dispersion, sodium molybdate and thioacetamide were added. The resulting mixture was placed in an autoclave and reacted at 200 °C for 18 h. The amounts of molybdenum source and sulfur source were adjusted to obtain CM¹, CM², CM³ and CM⁴ binary photocatalysts at the ratios of 10 mg/40 mg, 20 mg/80 mg, 30 mg/120 mg, and 40 mg/160 mg, respectively.

4. Preparation of bare MoS₂

In a typical procedure, 20 mg sodium molybdate and 80 mg thioacetamide were added into a mixed solvent

containing 20 mL diethylenetriamine (DETA) and 4 mL DI water. After stirring for 1 h, the solution was transferred into 50 mL Teflon-lined autoclave, sealed and heated at 200 °C for 18 h, and then allowed to cool to room temperature naturally. The resulting precipitates were collected by centrifuging, washed with ethanol and DI water three times until the organic molecules were completely removed, and then dried under vacuum at 60 °C overnight.^[2]

5. Preparation of CdS/MoS₂/Ag₂S nanodumbbells ternary heterostructure

The CdS/MoS₂/Ag₂S nanodumbbells heterostructures were synthesized through a cation exchange strategy using the CdS/MoS₂ (CM²) nanodumbbells as the precursor. Specifically, 100 mg CM² nanodumbbell catalyst was dispersed in 100 mL deionized water under ultrasonic treatment. Then, 0.2 mL AgNO₃ aqueous solution (0.01 M) was added into the above suspension, vigorously stirred for 30 min, the samples precipitate and are centrifuged, washed and dried overnight at 60 °C. The obtained sample is labeled as CMA.

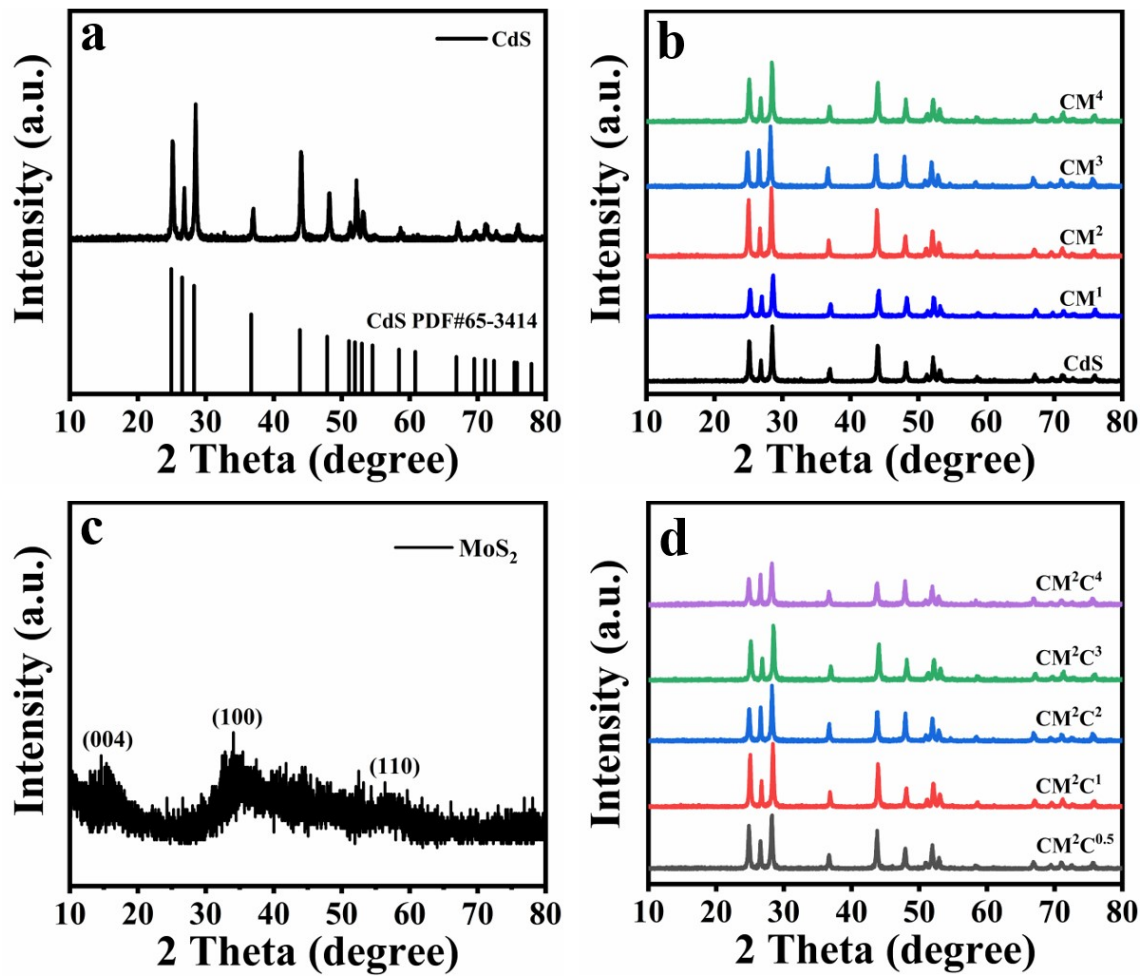


Figure S1. XRD patterns of (a) CdS, (b) CM^x (x=1, 2, 3, 4), (c) MoS₂, and (d) CM²C^x (x=0.5, 1, 2, 3, 4).

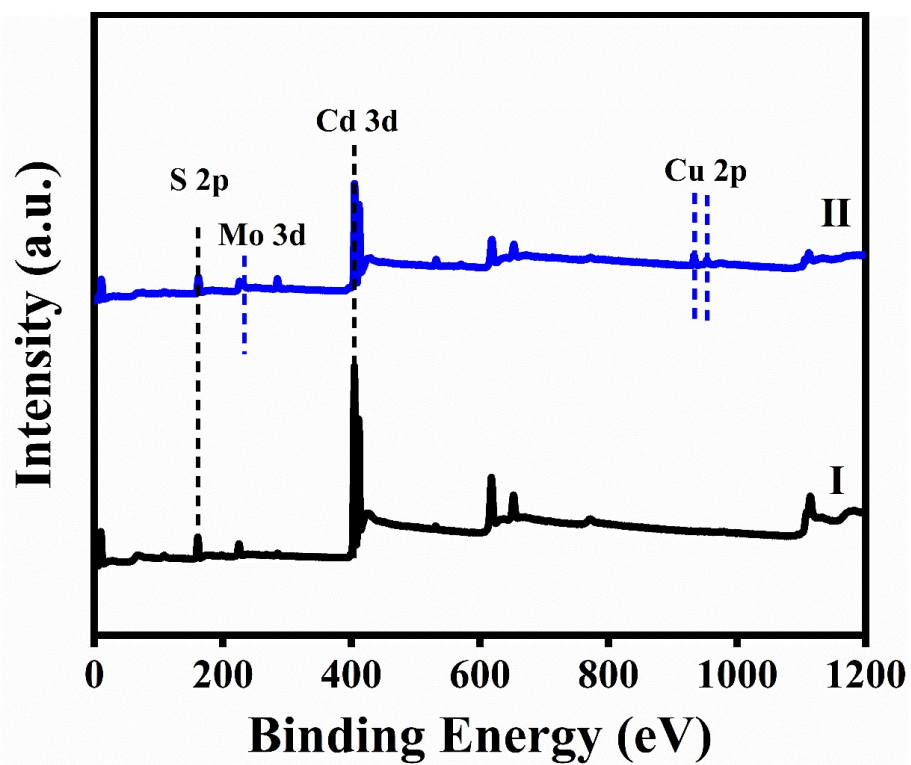


Figure S2. Survey spectrum of (I) CdS and (II) CM²C¹.

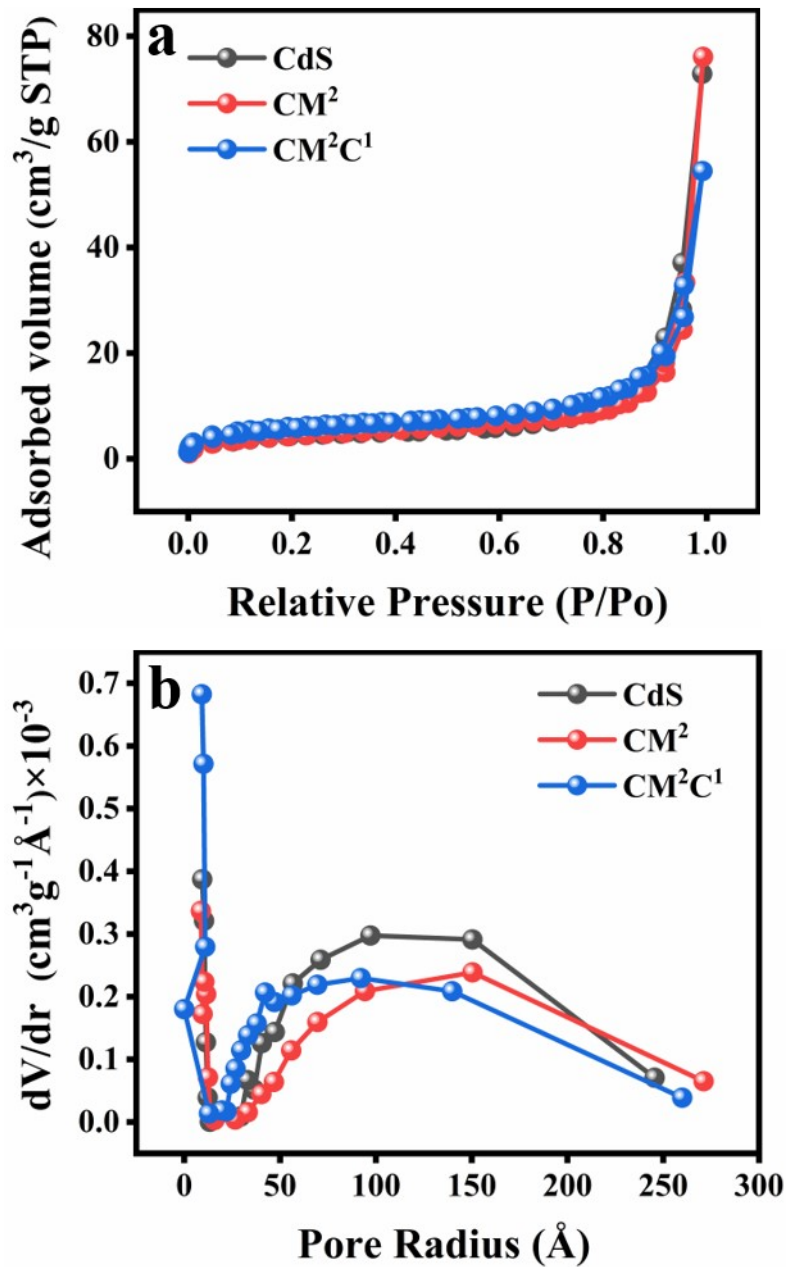


Figure S3. BET results of CdS, CM^2 and CM^2C^1 .

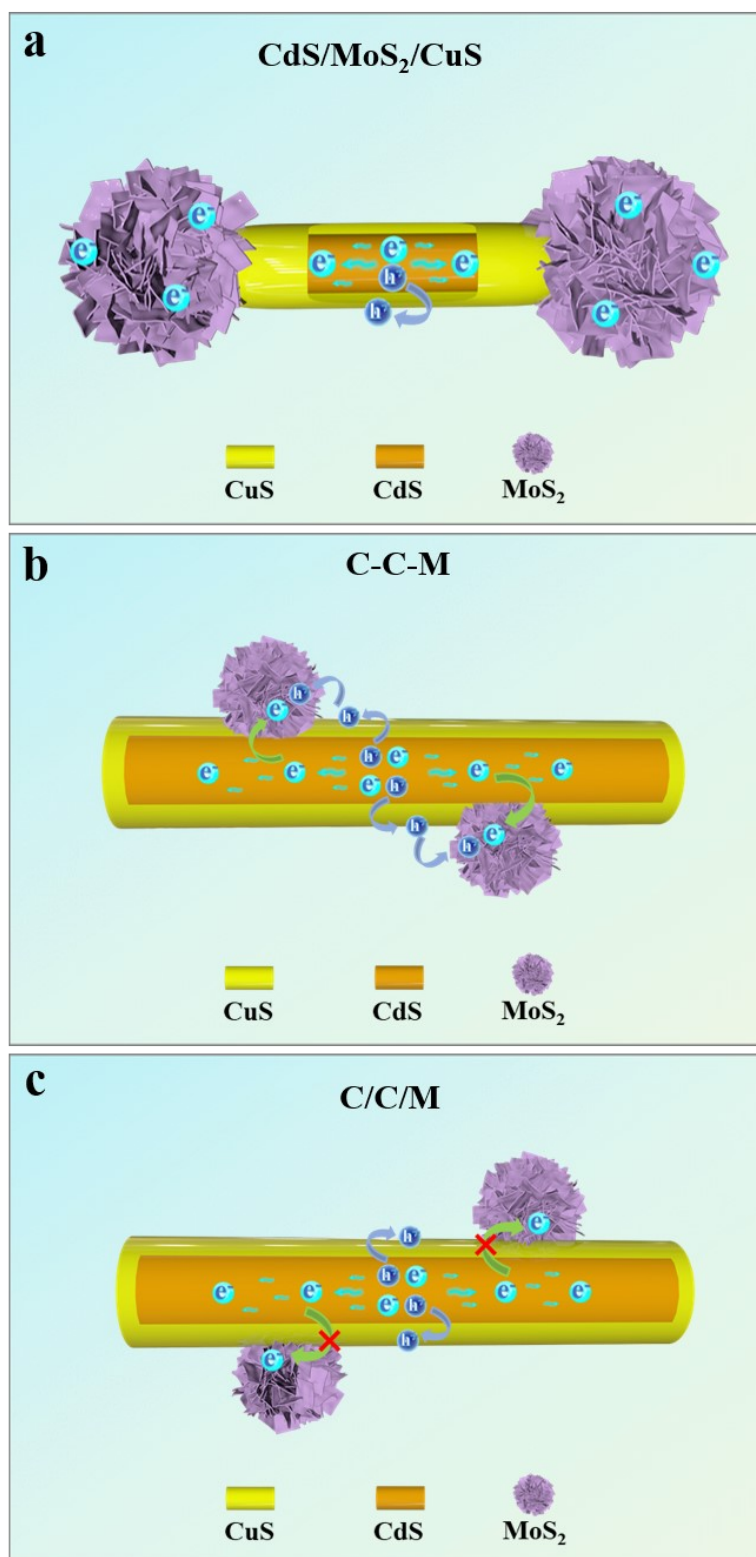


Figure S4. Schematic diagram of photoelectron transfer over the (a) CdS/MoS₂/CuS, (b) C-C-M and (c) C/C/M heterostructure.

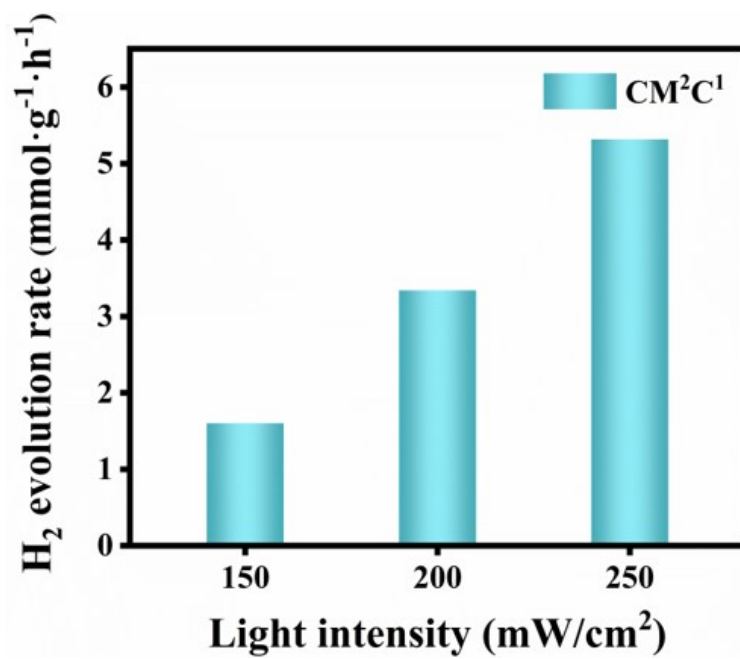


Figure S5. Photoactivities of CM²C¹ under different light intensity.

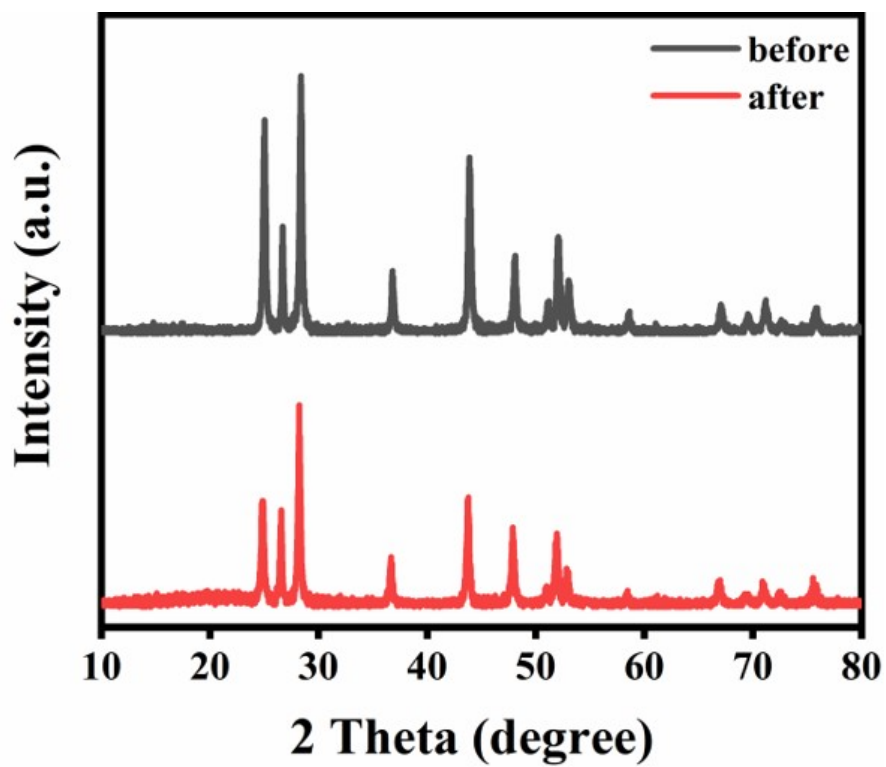


Figure S6. (a) XRD spectra of CM²C¹ before and after cyclic reaction.

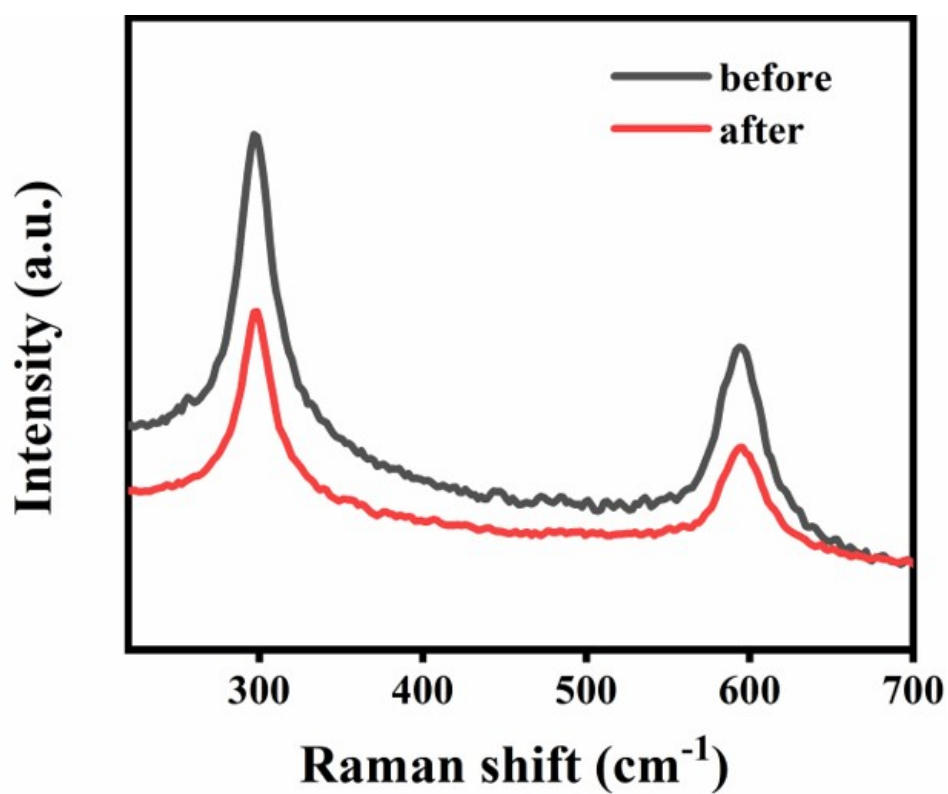


Figure S7. (a) Raman spectra of CM²C¹ before and after cyclic reaction.

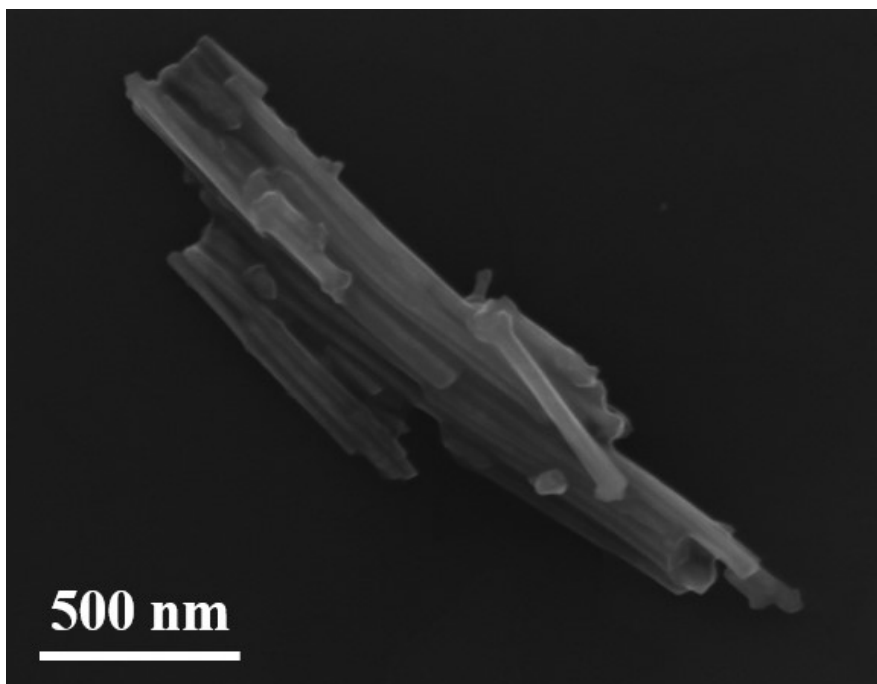


Figure S8. (a) SEM spectra of CM²C¹ after cyclic reaction.

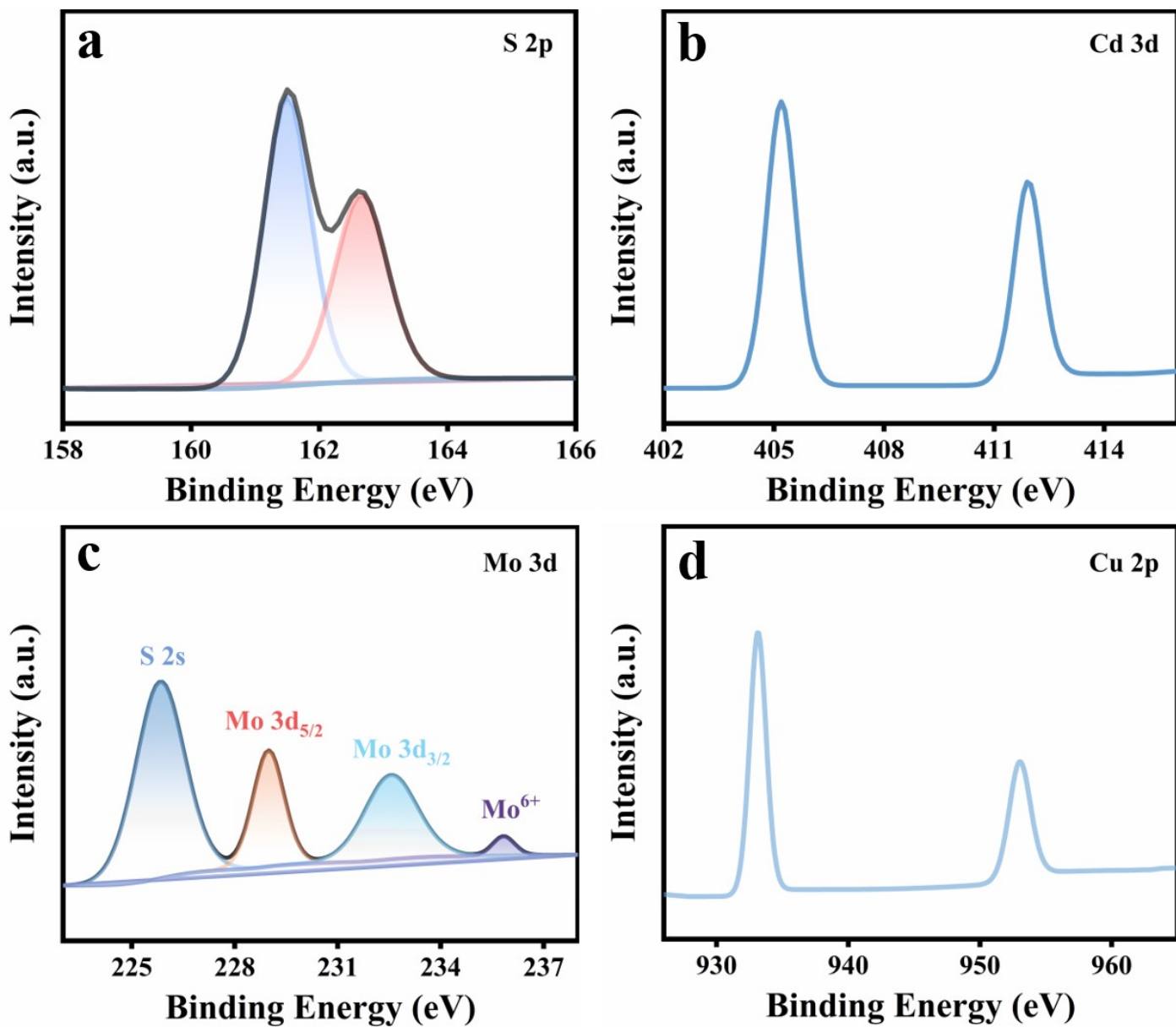


Figure S9. High-resolution (a) S 2p, (b) Cd 3d, (c) Mo 3d and (d) Cu 2p spectra of CM²C¹ after cyclic reaction.

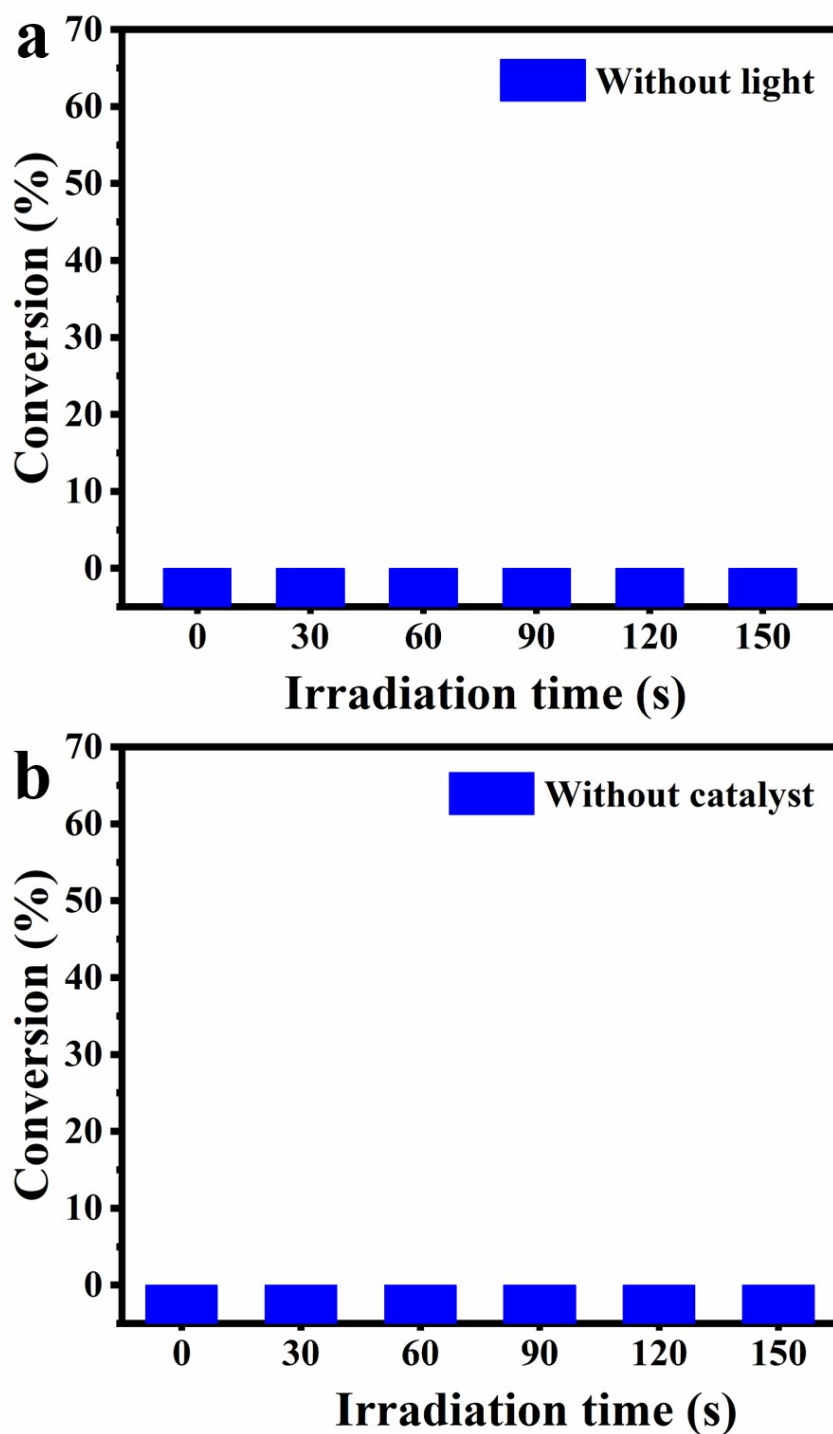


Figure S10. Blank experiments for photocatalytic reduction of 4-NA (a) without catalyst or (b) light irradiation.

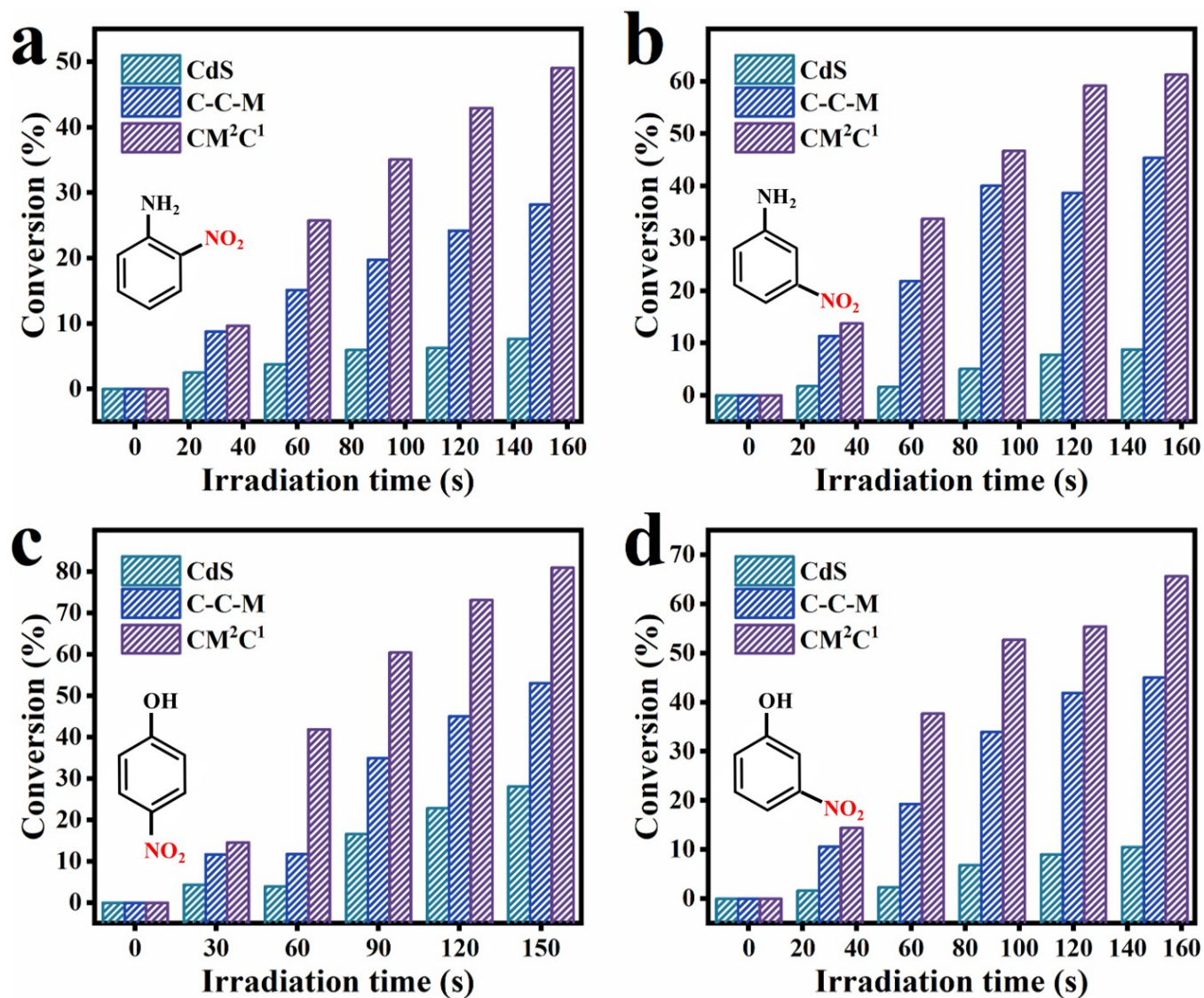


Figure S11. Photoactivities of CdS, C-C-M, and CM²C¹ towards the photoreduction of (a) 2-NA, (b) 3-NA, (c) 4-NP and (d) 3-NP.

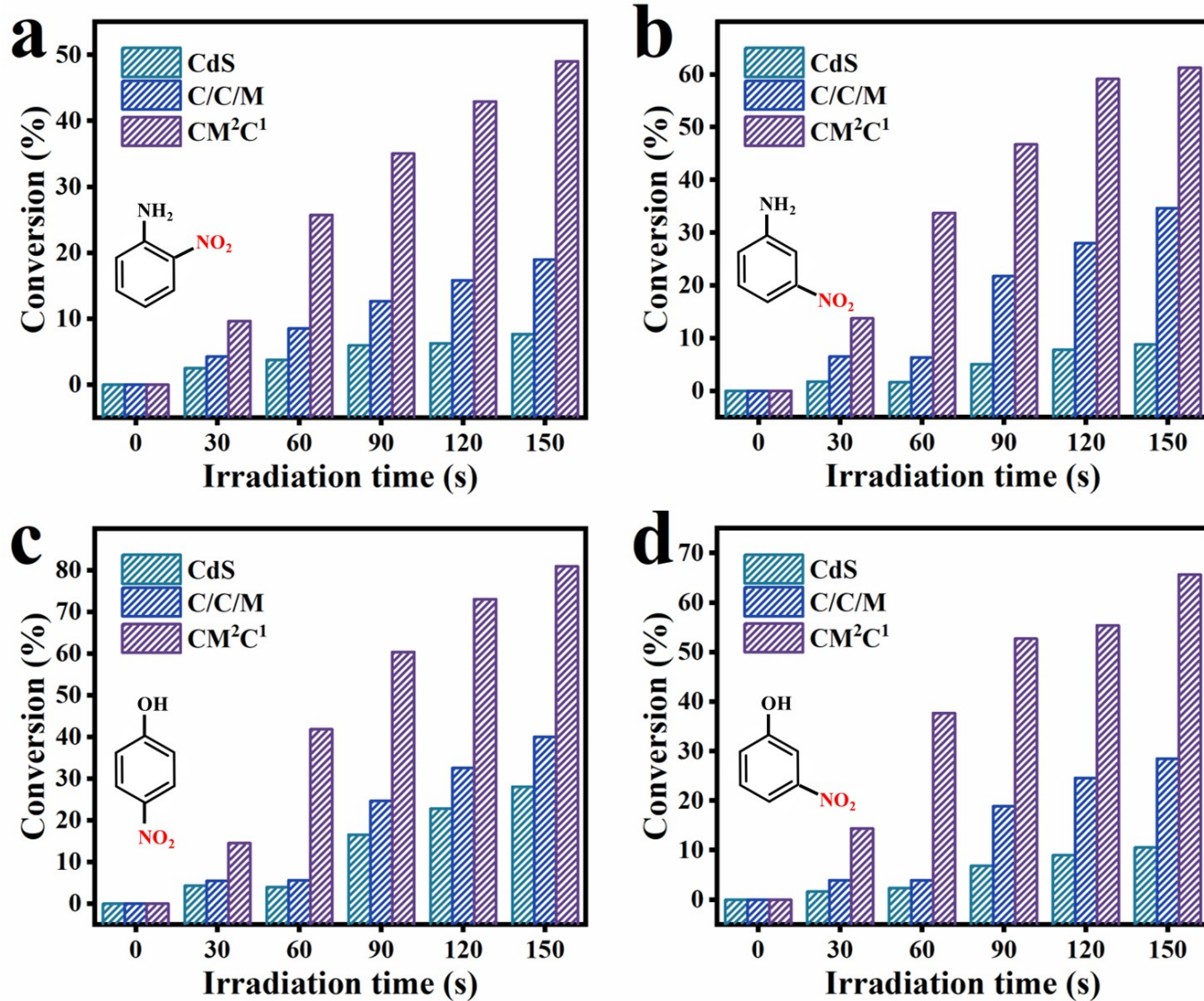


Figure S12. Photoactivities of CdS, C/C/M, and CM²C¹ towards photoreduction of (a) 2-NA, (b) 3-NA, (c) 4-NP and (d) 3-NP.

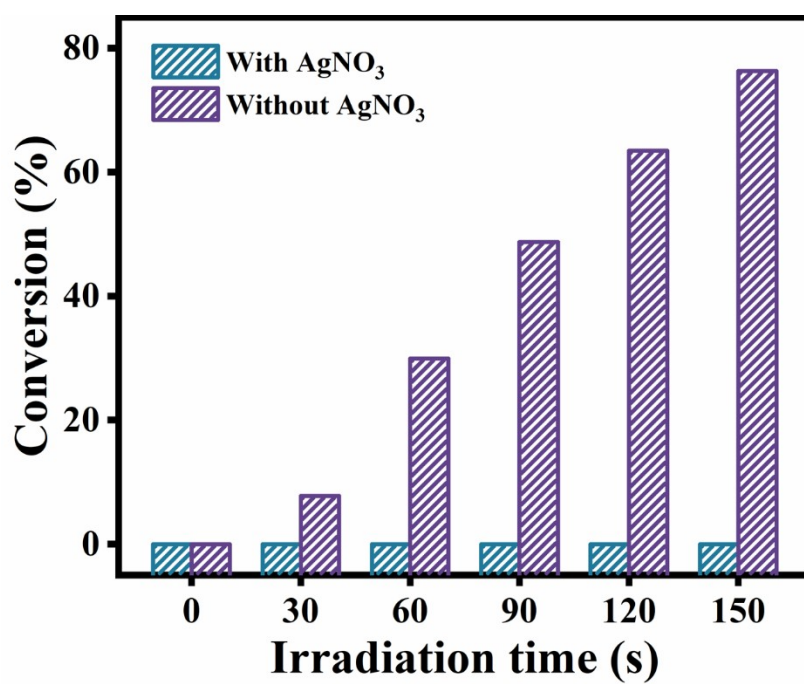


Figure S13. Photoactivities of CM²C¹ towards photoreduction of 4-NA with and without adding AgNO₃ as the electron scavenger.

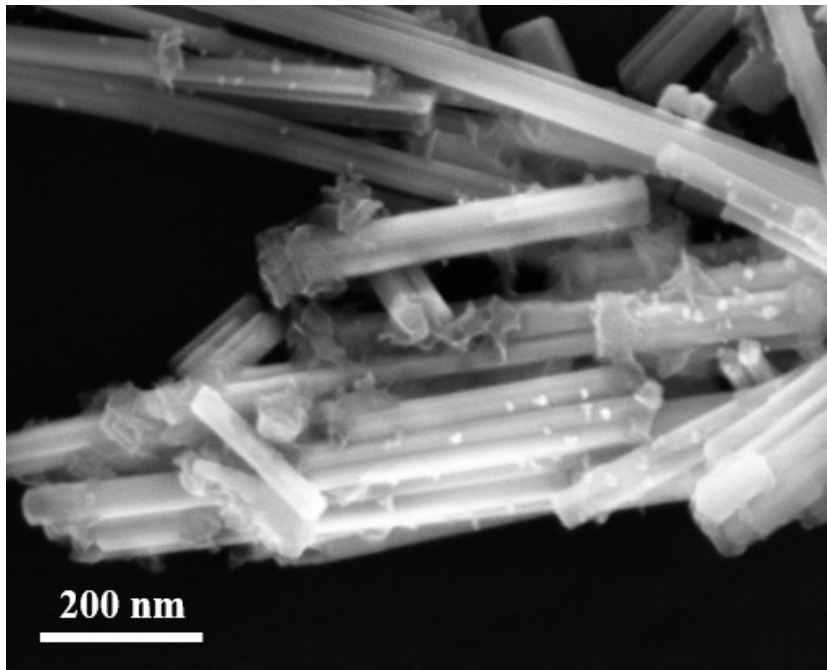


Figure S14. SEM image of CMA.

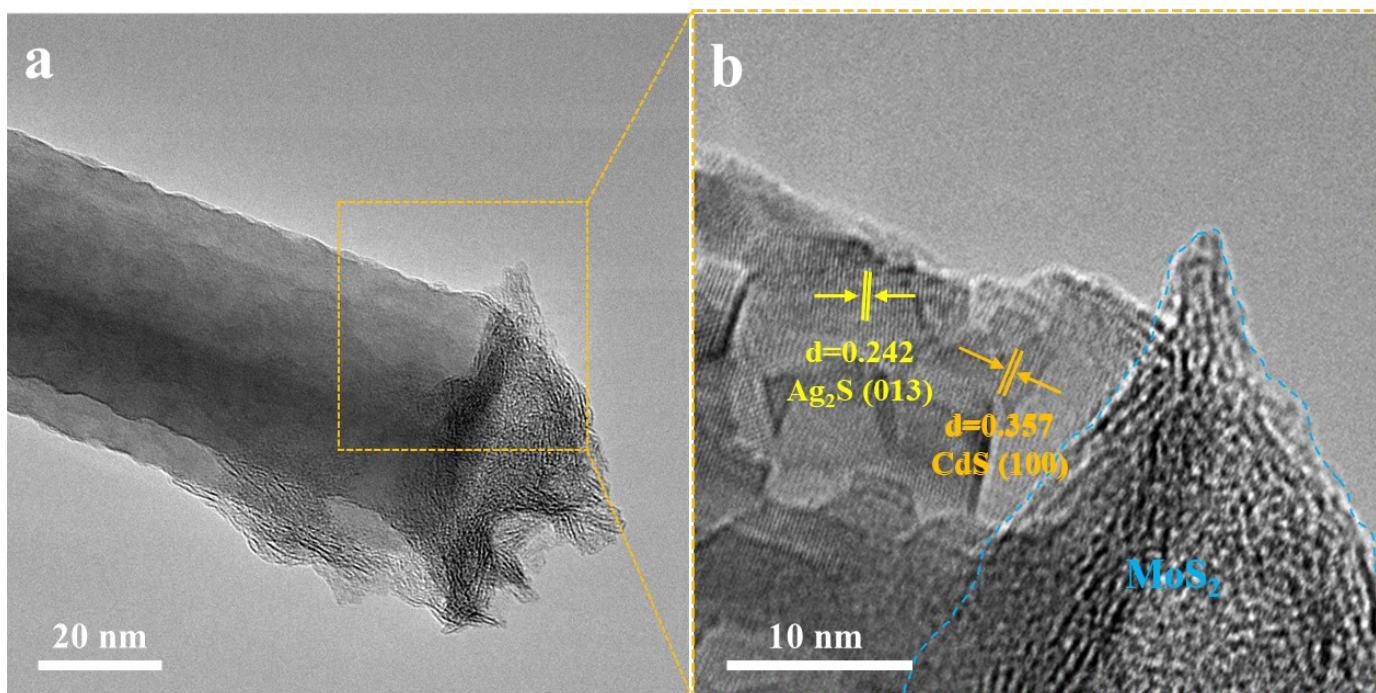


Figure S15. (a) TEM and (b) HRTEM image of CMA.

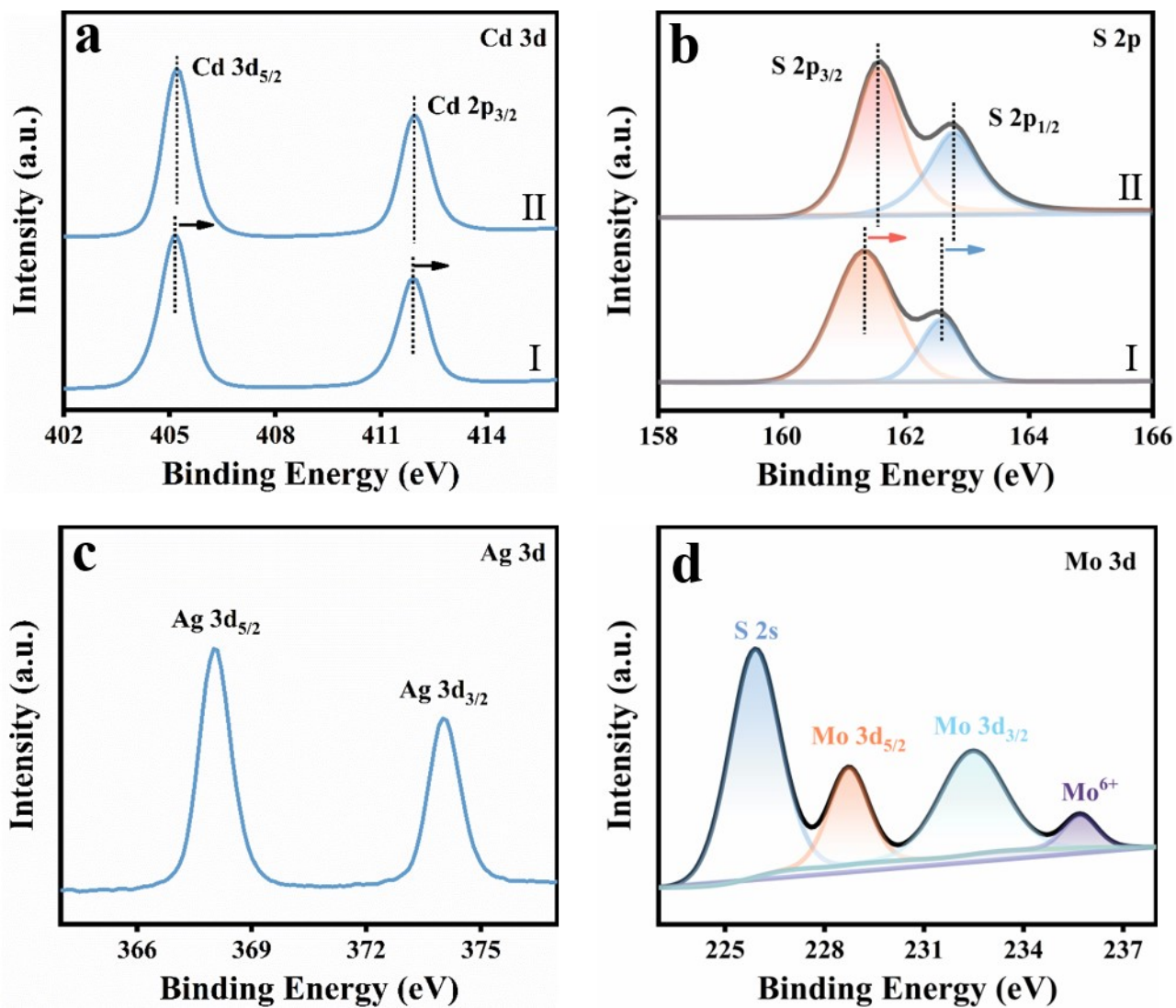


Figure S16. High-resolution (a) Cd 3d, (b) S 2p of (I) CdS and (II) CMA; high-resolution (h) Ag 3d and (i) Mo 3d of CMA.

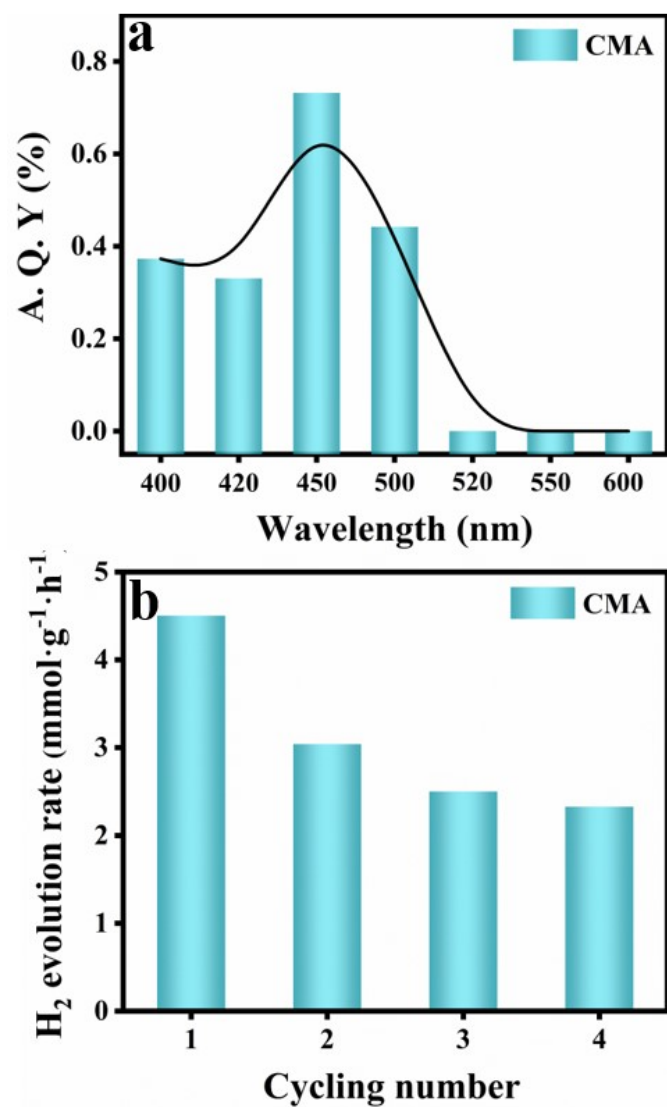


Figure S17. (a) A.Q.Y result of CMA under monochromatic light irradiation; (b) photostability of CMA.

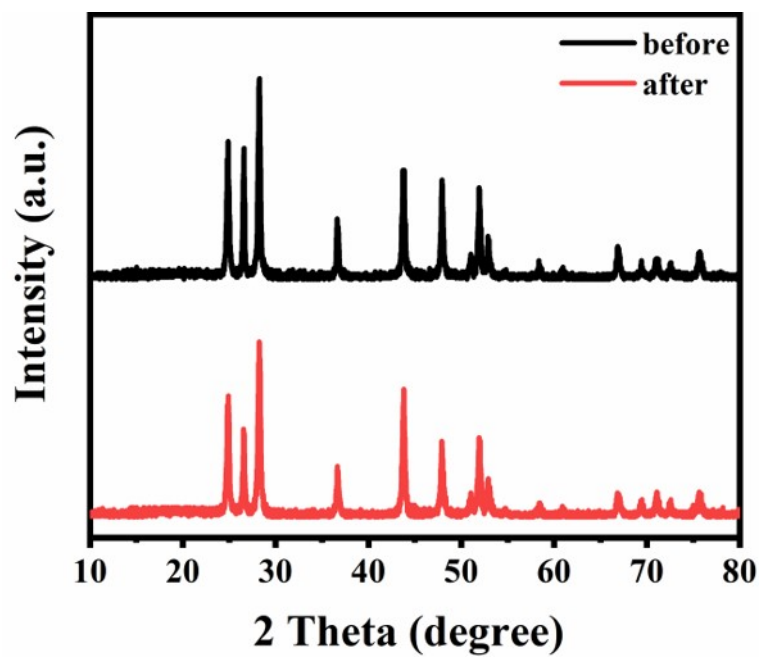


Figure S18. (a) XRD spectra of CMA before and after cyclic reaction.

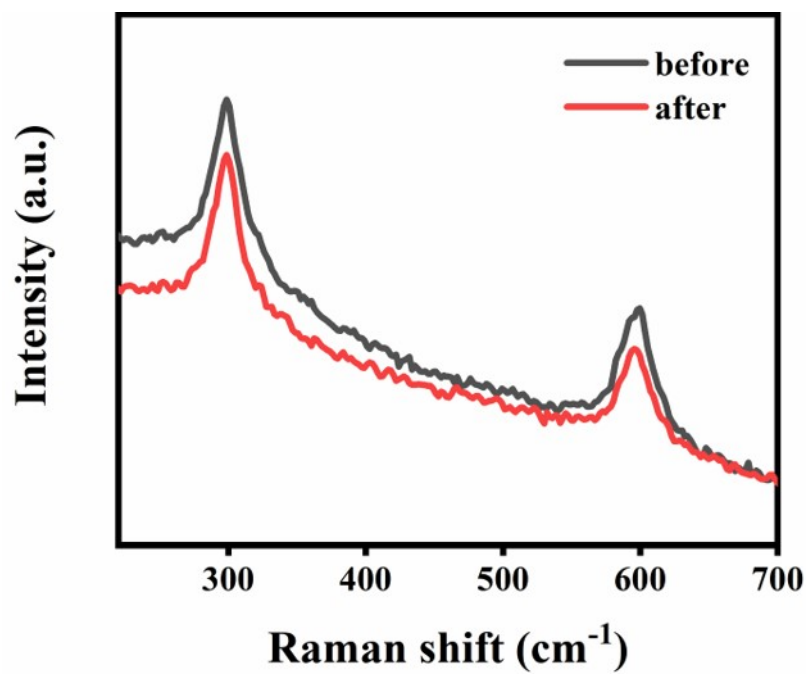


Figure S19. (a) Raman spectra of CMA before and after cyclic reaction.

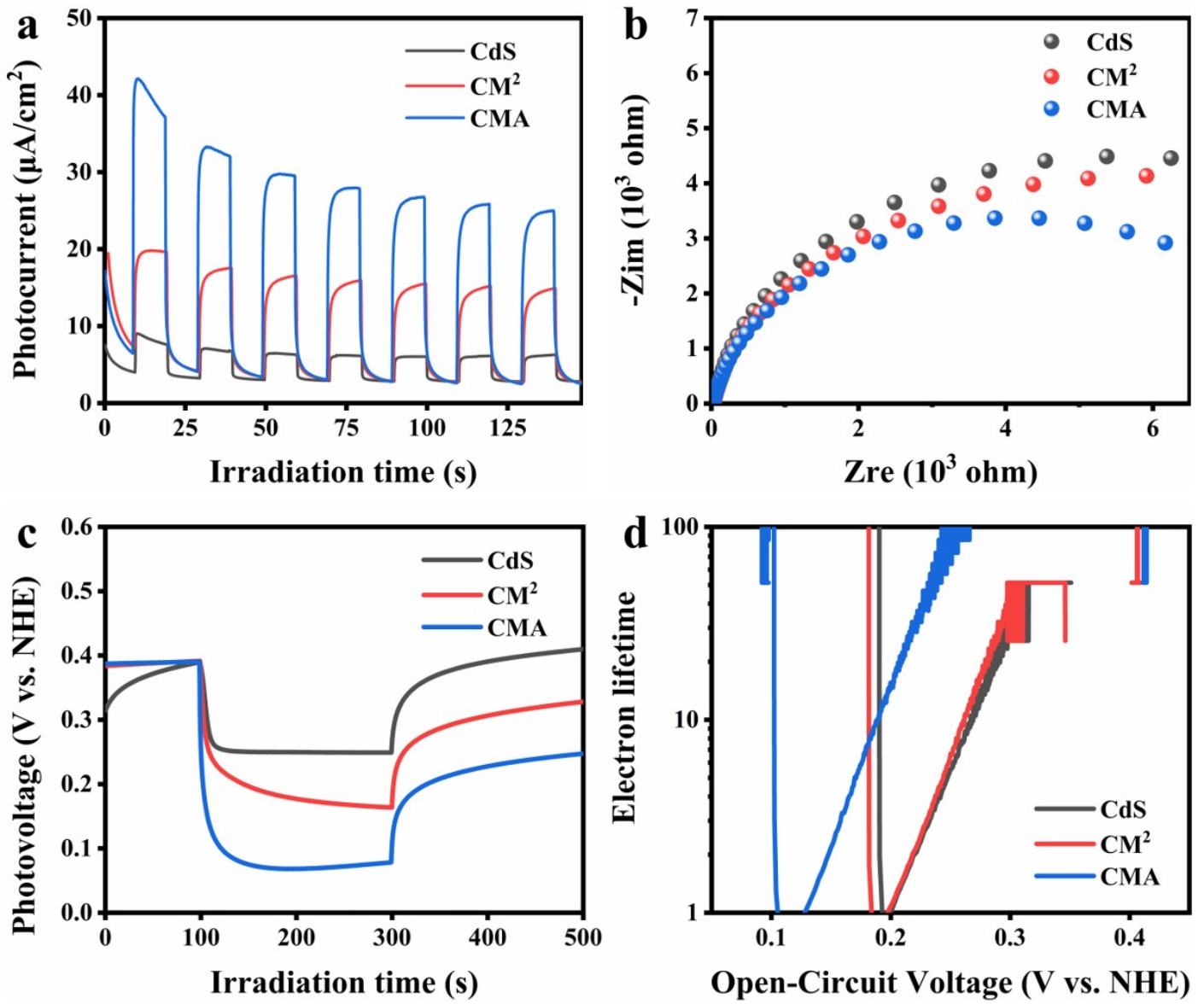


Figure S20. (a) I-t, (b) EIS (c) OCVD and (d) electron lifetime of CdS, CM² and CMA under visible light ($\lambda > 420 \text{ nm}$) irradiation.

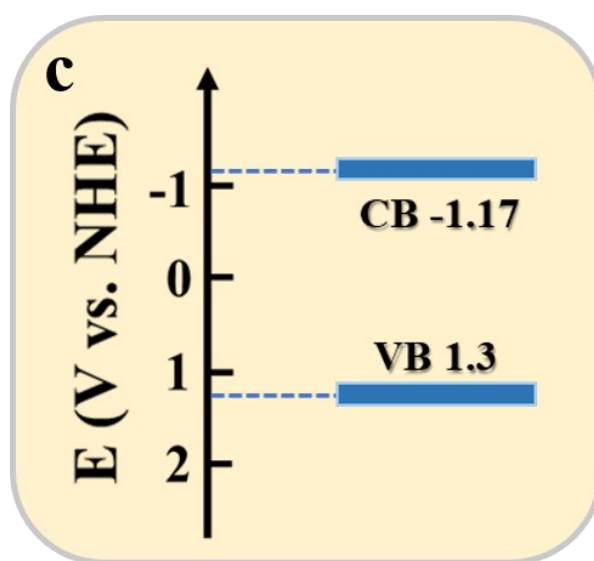
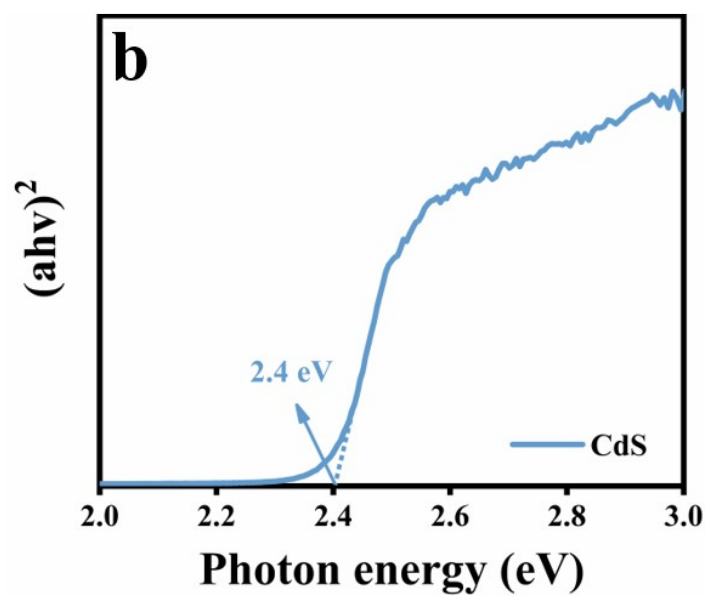
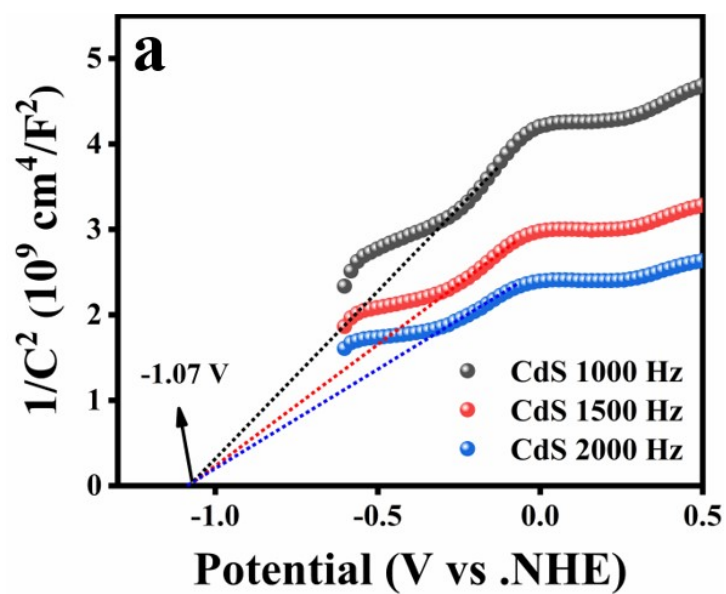


Figure S21. (a) M-S results, (b) bandgap determination, and (c) diagram showing the energy levels of CdS.

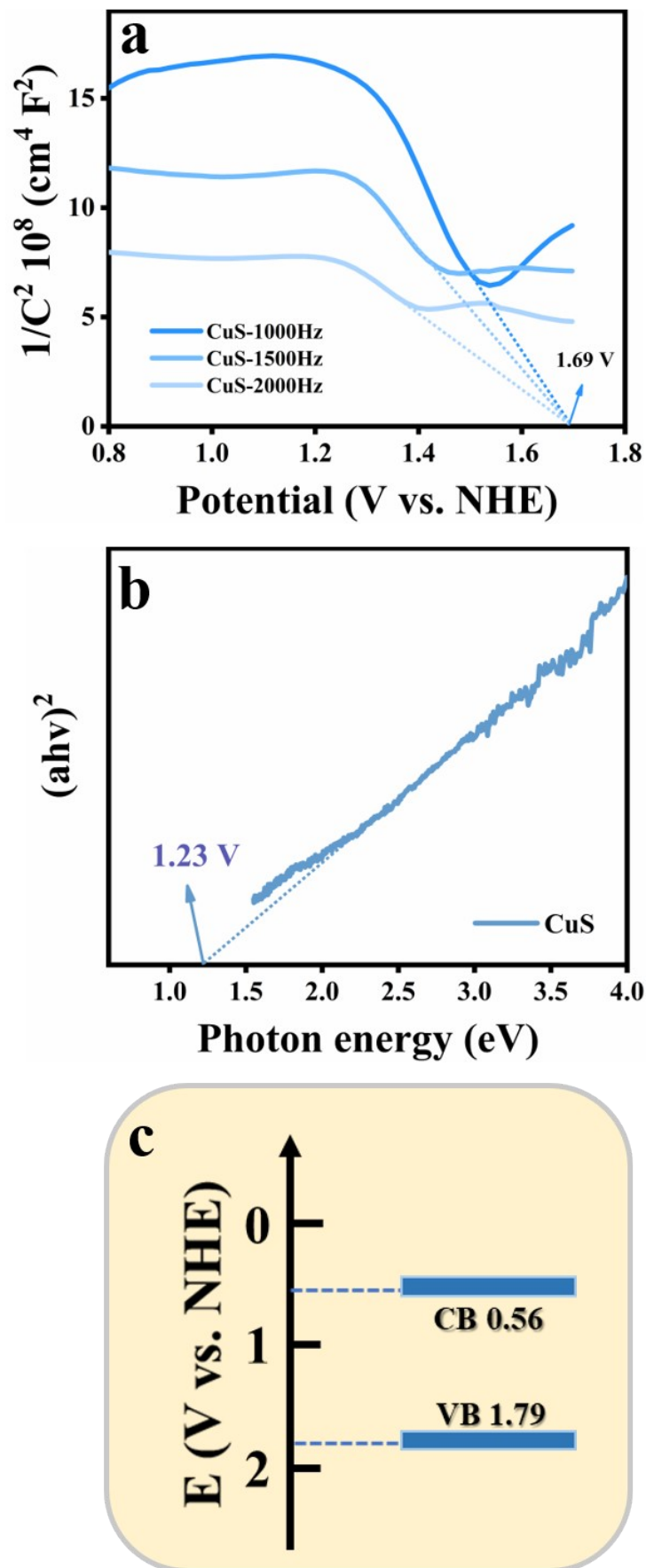


Figure S22. (a) M-S results, (b) bandgap determination, and (c) diagram showing the energy levels of CuS.

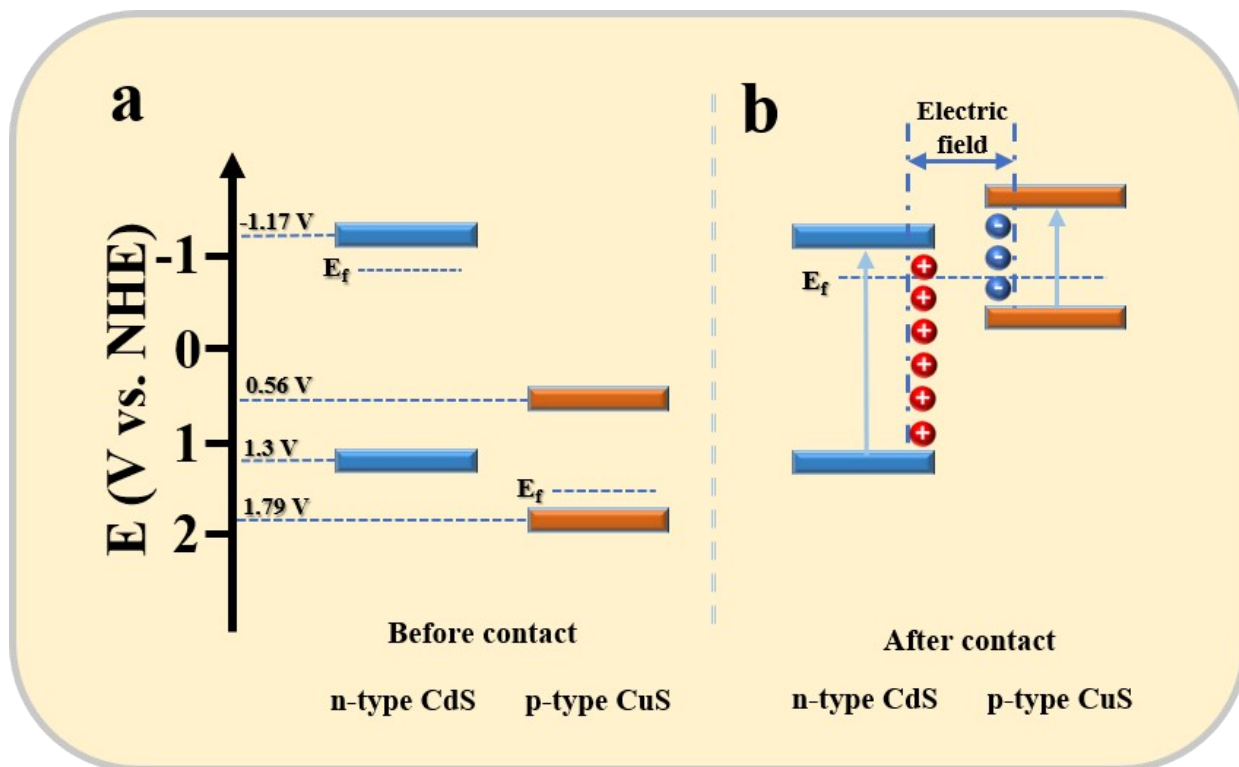


Figure S23. Energy band diagram of CdS/CuS heterostructure before and after contact.

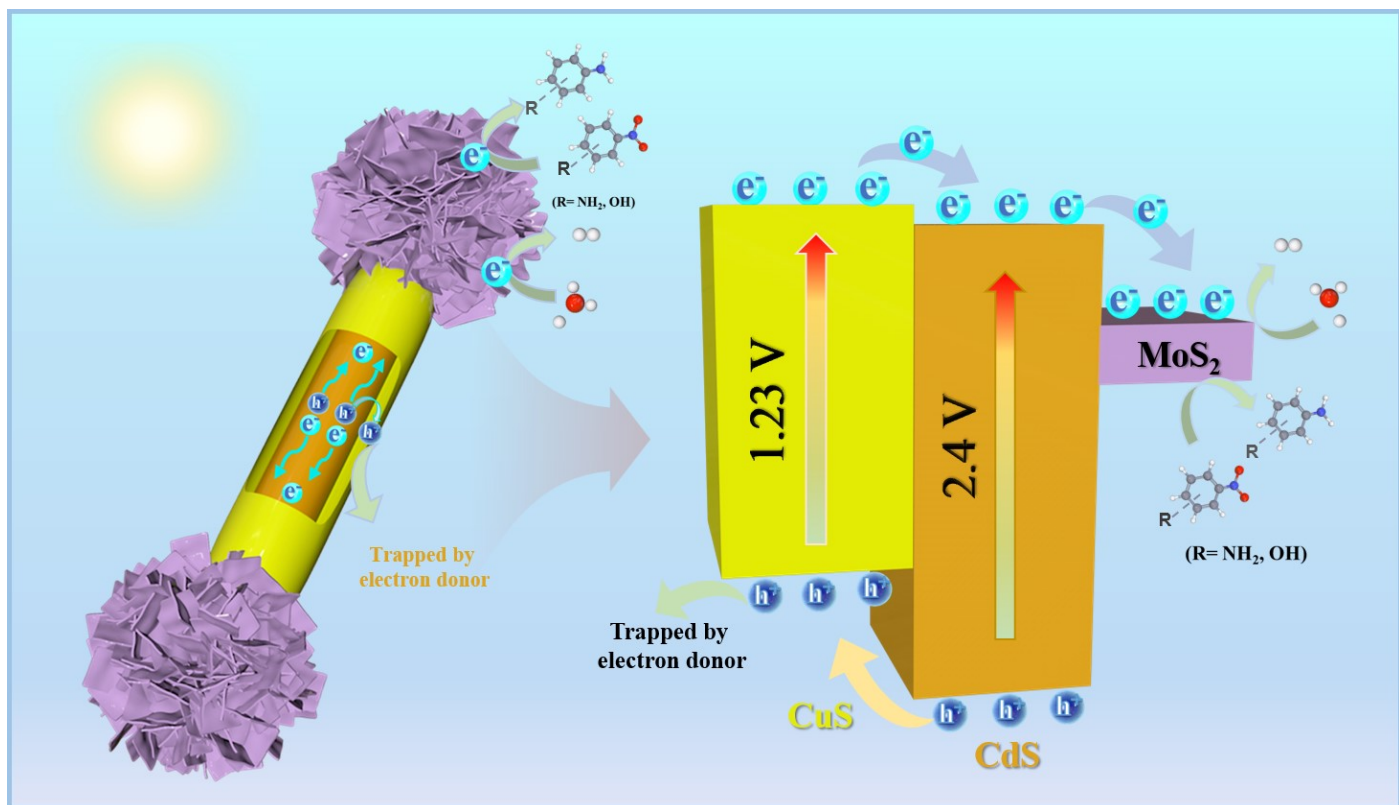


Figure S24. Schematic illustration of the photocatalytic mechanism of CdS/MoS₂/CuS heterostructure.

Table S1. Peak position with corresponding functional groups for CM²C¹ and CdS.

<i>Peak position (cm⁻¹)</i>	<i>CM²C¹</i>	<i>CdS</i>
3435	N-H stretching vibration	N-H stretching vibration ^[3]
1637	O-H deformation vibration	O-H deformation vibration ^[4]
2927 & 2848	-CH ₂ - stretching vibration	-CH ₂ - stretching vibration ^[5]

Table S2. Chemical bond species for different photoelectrodes.

<i>Element</i>	<i>CdS (eV)</i>	<i>CM²C¹</i>	<i>Chemical Bond Specie</i>
S 2p_{1/2}	162.6	162.65	S ^{2-[2, 6]}
S 2p_{3/2}	161.37	161.5	S ^{2-[2, 6]}
Cd 3d_{3/2}	411.89	411.95	Cd ^{2+[7]}
Cd 3d_{5/2}	405.16	405.21	Cd ^{2+[7]}
Cu 2p_{1/2}	/	953.05	Cu ^{2+[8]}
Cu 2p_{3/2}	/	933.16	Cu ^{2+[8]}
Mo 3d_{5/2}	/	228.93	Mo ^{4+[9]}
Mo 3d_{3/2}	/	232.27	Mo ^{4+[9]}
Mo 3d_{3/2}	/	235.88	Mo ^{6+[10]}
S 2s	/	225.87	S ^{2-[1]}

Table S3. Specific surface area, pore volume and pore size of CdS, CM² and CM²C¹.

<i>Samples</i>	<i>SBET (m²/g)^a</i>	<i>Total pore volume (cm³/g)^b</i>	<i>Average pore size (nm)^c</i>
<i>CdS</i>	<i>14.47</i>	<i>0.11</i>	<i>11.03</i>
<i>CM²</i>	<i>14.79</i>	<i>0.11</i>	<i>8.12</i>
<i>CM²C¹</i>	<i>20.00</i>	<i>0.08</i>	<i>10.49</i>

Table S4. Comparison on the photocatalytic activity of this work with the previously reported CdS-based Photocatalytic systems.

<i>Number</i>	<i>Materials</i>	<i>Sphere</i>	<i>Light source</i>	<i>Sacrificial reagent</i>	<i>Activity ($\mu\text{mol/g/h}$)</i>	<i>Reference</i>
This work	CdS/MoS ₂ /CuS	dumbbell-shaped	Visible light ($\lambda > 420 \text{ nm}$)	0.25 M Na ₂ S and 0.35 M Na ₂ SO ₃	4075	/
1	CdS/CoOx	core-shell nanorods	Visible light ($\lambda > 420 \text{ nm}$)	0.35 M Na ₂ S and 0.25 M Na ₂ SO ₃	3500	Appl. Catal. B Environ. Energy, 2018, 234, 109-116.
2	5.0%-Ag ₂ S/CdS	nanowires	Visible light ($\lambda > 420 \text{ nm}$)	2 vol% lactic acids	777	RSC Adv., 2021, 11, 28211-28222.
3	1% CSs/CdS	spheres	Visible light ($\lambda > 420 \text{ nm}$)	0.5 M Na ₂ S and 0.5 M Na ₂ SO ₃	3887	Catal. Today, 2017, 281, 662-668.
4	NiPx/MoS ₂ /NiS/CdS	nanowires	Visible light ($\lambda > 400 \text{ nm}$)	5 g/L glucose	297	J. Am. Ceram. Soc., 2021, 104, 5307-5316.
5	g-C ₃ N ₄ /CdS/NiS	nanorods	Visible light ($\lambda > 420 \text{ nm}$)	10% triethanolamine	2563	J. Mater. Chem. A, 2015, 3, 18244-18255.
6	NiS/CdS/h-TiO ₂	nanosheets	Visible light ($\lambda > 420 \text{ nm}$)	0.35 M Na ₂ S and 0.25 M Na ₂ SO ₃	2149	Appl. Surf. Sci., 2019, 476, 378-386.
7	2%Ni ₂ P/CdS NRs	nanorods	Visible light ($\lambda > 400 \text{ nm}$)	Na ₂ S and Na ₂ SO ₃	2602	Catalysts, 2022, 12, 417.
8	3DOM TiO ₂ -Au-CdS	nanoparticles	Visible light ($\lambda > 400 \text{ nm}$)	0.1 M Na ₂ S and 0.1 M Na ₂ SO ₃	3500	Nano Energy, 2018, 47, 266-274.
9	CdS/Ni-MOF (40)	spheres	Visible light ($\lambda > 420 \text{ nm}$)	6% lactic acid	2508	Appl. Surf. Sci., 2020, 522, 146356.
10	CdS-Ag ₂ S	Hierarchically nanostructured	Visible light ($\lambda > 420 \text{ nm}$)	10% triethanolamine	380	Appl. Surf. Sci., 2019, 470, 196-204.

Table S5. Chemical bond species for different photoelectrodes.

<i>Element</i>	<i>CdS (eV)</i>	<i>CMA</i>	<i>Chemical Bond Specie</i>
S 2p_{1/2}	162.6	162.79	S ^{2-[2, 6]}
S 2p_{3/2}	161.37	161.57	S ^{2-[2, 6]}
Cd 3d_{3/2}	411.89	411.94	Cd ^{2+[7]}
Cd 3d_{5/2}	405.16	405.21	Cd ^{2+[7]}
Ag 2p_{3/2}	/	374.03	Cu ^{2+[11]}
Ag 2p_{5/2}	/	368.04	Cu ^{2+[11]}
Mo 3d_{5/2}	/	228.93	Mo ^{4+[9]}
Mo 3d_{3/2}	/	232.27	Mo ^{4+[9]}
Mo 3d_{3/2}	/	235.88	Mo ^{6+[10]}
S 2s	/	225.87	S ^{2-[1]}

References

- [1] L. Zhang, X. Jiang, Z. Jin and N. Tsubaki, Spatially Separated Catalytic Sites Supplied with CdS-MoS₂-In₂O₃ Ternary Dumbbell S-scheme heterojunction For Enhanced Photocatalytic Hydrogen Production, *J. Mater. Chem. A*, **2022**, 10, 10715-10728.
- [2] B. Qiu, L. Cai, N. Zhang, X. Tao and Y. Chai, A Ternary Dumbbell Structure with Spatially Separated Catalytic Sites for Photocatalytic Overall Water Splitting, *Adv. Sci.*, **2020**, 7, 1903568.
- [3] K. Wang, X. Z. Ge, Q. L. Mo, X. Yan, Y. Xiao, G. Wu, S. R. Xu, J. L. Li, Z. X. Chen and F. X. Xiao, Steering bi-directional charge transfer via non-conjugated insulating polymer, *J. Catal.*, **2022**, 416, 92-102.
- [4] P. Su, B. Tang and F. X. Xiao, Layer-By-Layer Assembly of Atomically Precise Alloy Nanoclusters Photosystems for Solar Water Oxidation, *Small*, **2024**, 20, 2307619.
- [5] Q. L. Mo, S. R. Xu, J. L. Li, X. Q. Shi, Y. Wu and F. X. Xiao, Solar-CO₂-to-Syngas Conversion Enabled by Precise Charge Transport Modulation, *Small*, **2023**, 19, 2300804.
- [6] X. X. Lu, W. J. Chen, Y. Yao, X. M. Wen, J. N. Hart, C. Tsounis, C. Y. Toe, J. Scott and Y. H. Ng, Photogenerated charge dynamics of CdS nanorods with spatially distributed MoS₂ for photocatalytic hydrogen generation, *Chem. Eng. J.*, **2021**, 420, 127709.
- [7] Y. Li, Q. Zhao, Y. Zhang, Y. Li, L. Fan, F.-t. Li and X. Li, In-situ construction of sequential heterostructured CoS/CdS/CuS for building “electron-welcome zone” to enhance solar-to-hydrogen conversion, *Appl. Catal., B*, **2022**, 300, 120763.
- [8] Y. L. Han, X. F. Dong and Z. B. Siang, Synthesis of MnxCd_{1-x}S nanorods and modification with CuS for extraordinarily superior photocatalytic H₂ production, *Catal. Sci. Technol.*, **2019**, 9, 1427-1436.
- [9] G. Eda, H. Yamaguchi, D. Voiry, T. Fujita, M. W. Chen and M. Chhowalla, Photoluminescence from Chemically Exfoliated MoS₂, *Nano Lett.*, **2011**, 11, 5111-5116.
- [10] J. Y. Tang, Y. P. Shi, W. Cai and F. L. Liu, Construction of Embedded Heterostructured SrZrO₃/Flower-like MoS₂ with Enhanced Dye Photodegradation under Solar-Simulated Light Illumination, *Acs Omega*, **2020**, 5, 9576-9584.
- [11] L. Deng, D. Yin, K. K. Khaing, S. Xiao, L. Li, X. Guo, J. Wang and Y. Zhang, The facile boosting sunlight-driven photocatalytic performance of a metal-organic-framework through coupling with Ag₂S nanoparticles, *New J. Chem.*, **2020**, 44, 12568-12578.